International Journal of Science and Research Archive

eISSN: 2582-8185

Cross Ref DOI: 10.30574/ijsra

Journal homepage: https://ijsra.net/

(RESEARCH ARTICLE)

Check for updates

Evaluation of sand characterization (XRF/XRD/TGA) on the structural performance and thermal stability of deep beams

Oluwaseun Samuel Oguntoye *, Lekan Makanjuola Olanitori, Samuel Lambe Akingbonmire and Williams Ebhodaghe Egbele

Department of Civil and Environmental Engineering, School of Infrastructures, Minerals and Manufacturing Engineering, The Federal University of Technology Akure, Nigeria.

International Journal of Science and Research Archive, 2026, 19(01), 1008-1021

Publication history: Received on 15 March 2026; revised on 22 April 2026; accepted on 24 April 2026

Article DOI: https://doi.org/10.30574/ijsra.2026.19.1.0872

Abstract

Deep beams are critical structural elements in reinforced concrete design, yet their complex stress distribution and strength behavior under varying loading conditions remain a challenge for engineers. This study investigates the influence of sand characterization on the mechanical and thermal performance of deep beams. Three sand samples (A, B, and C) were analyzed using sieve analysis, moisture content determination, compressive strength testing, X-ray fluorescence (XRF), X-ray diffraction (XRD), and Thermogravimetric analysis (TGA). Concrete specimens (I, J, and K) were prepared from each sand type and tested at 7, 14, 21 and 28 days of curing. Results revealed that Sand B, with the lowest silt fines content (4.95%) and highest fineness modulus (3.79), produced concrete Sample J with superior compressive strength of 20.29 N/mm^2 at 28 days and characteristic strength of 16.98 N/mm^2. XRF confirmed silica dominance with concentration of 66% to 74% in fine aggregates, while XRD highlighted Sand B's high quartz content of 64 wt.%. TGA demonstrated enhanced thermal stability in Sample J, with reduced mass loss and improved fire resistance. These findings underscore the importance of aggregate characterization in optimizing deep beam performance, particularly under high-temperature conditions, and provide insights for safer, more durable structural design.

Keywords: Deep Beams; Characterization; Compressive strength; Thermal stability

1. Introduction

Concrete deep beams are structural members with a span-to-depth ratio less than two, making them distinct from conventional shallow beams. Unlike slender beams, deep beams exhibit nonlinear stress distribution, with load transfer occurring through compression struts rather than flexural action. The strain distribution in deep beams is not linear across the transverse section as in the elementary beam theory. It is because that the transfer of load is happening mainly through the arch action (ACI-318, 2008) So, the traditional beam theory cannot be used for deep beams [1].

According to BS 8110-1:1997, a deep beam is defined as a beam in which the effective span (L_e) is less than or equal to: two times the overall depth (h) for a simply supported beam (Le < 2h) and two and a half times the overall depth (h) for a continuous beam (Le < 2.5h) with a length ratio ranging between 0.5 to 2.0 [2].

Reinforced concrete deep beams are mainly used in massive application in various civil engineering structures, such as transfer girders in tall buildings, offshore structures, shear walls, wall footings, foundation pile caps and bridges [1]. Their application in high-rise buildings, bridges, and industrial structures necessitates a thorough understanding of their mechanical and thermal behavior.

* Corresponding author: Oluwaseun Samuel Oguntoye

Construction aggregate, or simply ‘aggregate’, is a broad category of particulate materials used in construction which includes sand (fine aggregate), and granite (coarse aggregates). One of the most critical factors influencing deep beam performance is the quality of fine aggregates (sand) used in concrete production. Sand contributes to the packing density, workability, and strength of concrete.

The evaluation of sand characterization using X-ray Fluorescence (XRF), X-ray Diffraction (XRD), and Thermogravimetric Analysis (TGA) is critical for determining the structural performance and thermal stability of high-performance concrete, particularly in deep beams where material consistency is paramount. These techniques help identify the mineralogical, chemical, and thermal properties of sand (natural or manufactured) to ensure high compressive strength, optimal interfacial transition zones (ITZ), and resistance to thermal degradation.

This research focuses on the characterization of three sand samples (A, B, and C) and their impact on the compressive strength and thermal resistance of deep beams. By employing advanced analytical techniques such as; XRF for chemical composition, XRD for mineralogical phases, and TGA/DTA for thermal degradation which makes the study bridges material science with structural engineering. The findings aim to guide engineers in selecting aggregates that enhance both mechanical strength and thermal resistance, thereby improving safety and durability in construction.

1.1. Statement of the problem

Deep beam design is often hindered by difficulties in modeling complex stress behaviors, a problem made worse by limited knowledge on how different sand types affect concrete. This study bridges that gap by investigating how specific silt contents and mineral compositions can be selected to improve the structural and thermal resilience of the concrete.

1.2. Objective of the study

This research focuses on the characterization of three sand samples (A, B, and C) and their impact on the compressive strength and thermal resistance of deep beams. By employing advanced analytical techniques XRF for chemical composition, XRD for mineralogical phases, and TGA/DTA for thermal degradation, the study bridges material science with structural engineering. The findings aim to guide engineers in selecting aggregates that enhance both mechanical strength and fire resistance, thereby improving safety and durability in construction.

2. Literature Review

2.1. Preamble

Structures in civil engineering consist of various components and elements which includes foundations, columns, beams, slabs etc. They are typically designed to withstand various loads they are meant to carry [3]. Failure sometimes is inevitable and can occur in one or more of these structural components. Hence, structural elements taking for instance reinforced concrete beams which span horizontally and transfer load from slab to the column usually need to be strengthened [4].

2.2. Concrete as a construction material

An important structural material in civil engineering construction is concrete. Concrete is a composite material mainly consisting of aggregates of different sizes embedded in mortar matrix. The mortar matrix has high porosity, and the pores are filled with air and water. A large number of bond micro-cracks exist at the interface between the coarse aggregates and the matrix. These properties strongly affect the complex nonlinear behavior of concrete [5]. Concrete is widely used in various building structures, which plays a very important role in the stability of the building structure and concrete itself has the irreplaceable advantages of other building materials [6]. The composite materials of concrete are cement, sand, gravel, and water, sometimes mixed with a small amount of various additives. These raw materials are successively mixed, cast, compacted, and cured, and gradually coagulated and hardened and, then, concrete is made. The main reason for concrete having complicated behavior is that concrete is a multiphase material of inhomogeneous and anisotropic and is varied with time and environmental conditions, as shown by the existing experimental investigation [7]. When a piece of concrete is sawn from a concrete structure, the internal non-uniform construction of concrete can be seen by the naked eye and the main compositions contained are as shown in Figure 1.

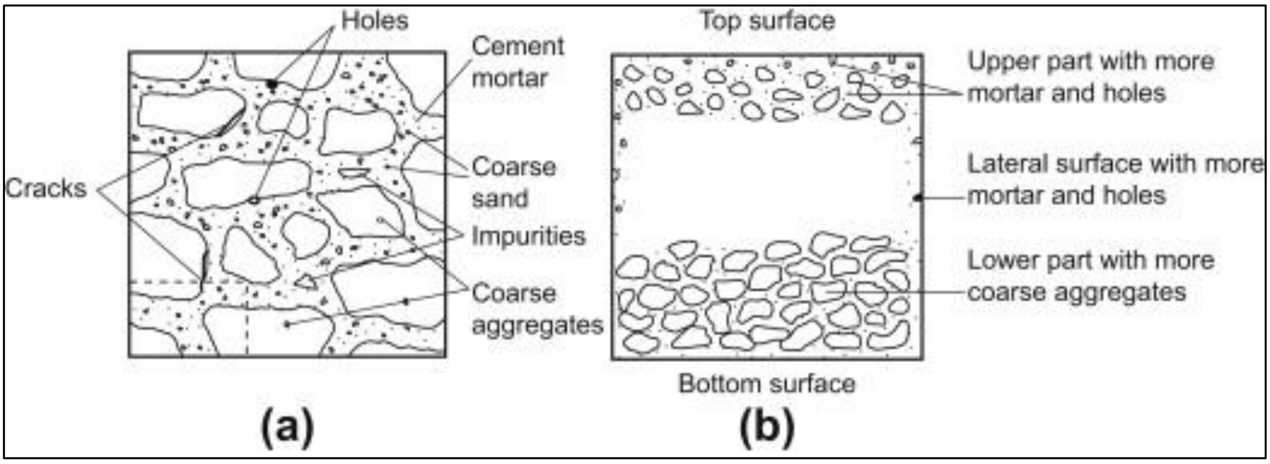

Figure 1 The internal non-uniform construction of concrete [7]

2.3. Deep Beams as a Structural Member

Deep beams are structural members characterized by their relatively large depth compared to their span [8, 9]. They are commonly used in various civil engineering applications, such as bridges, transfer girders, and foundation beams. Due to their unique geometry, DBs experience complex load distributions and stress patterns, requiring specialized design [10]. One of the primary challenges in designing deep beams is their ability to resist shear forces. Unlike regular beams, deep beams are more prone to shear failures due to the increased amount of shear stress developed in their span. Researchers have extensively studied the behavior of deep beams to develop effective design approaches and guidelines [11].

2.4. Role of Fine Aggregates in Concrete

The quality of sand is crucial to how deep beams perform. It dictates the concrete's workability, packing density, and strength. Furthermore, inconsistencies in sand's particle size, mineral makeup, or thermal stability can drastically change how a beam behaves under normal loads or extreme conditions like fire. Fine aggregates, typically sand (< 5mm), are vital in concrete, comprising 35-45% of the total volume to fill voids between coarse aggregates, increasing mix density. Their grading, shape, and mineral composition affect workability, density, and strength. [12] highlighted that well graded sands improve packing density, reducing voids and enhancing compressive strength. Sands with excessive fines (clay and silt) can impair bonding and increase shrinkage. Thus, characterization of sand is vital for predicting concrete performance. They improve workability, act as fillers, reduce porosity, and ensure a smooth surface finish. Properly graded fine aggregates minimize voids and increase the overall compressive strength. Fine aggregates function to fill the pores between coarse aggregates to minimize the air content in the concrete mixture so as not to reduce the strength of concrete due to the gradation and uniformity of the aggregate.

3. Materials and Methods

3.1. Materials

The materials used for this study were Ordinary Portland cement of grade 32.5 (binder), sand (fine aggregate), which is of three different sand samples named sample A, sample B, and sample C, were collected from different sources. Each sample was subjected to preliminary characterization tests to determine particle size distribution, silt fines content, and grading parameters. Crushed granite (coarse aggregate), high yield reinforcement bars, and potable water. The concrete grade is C20/25, while the yield stress for the reinforcement bar is 410 N/mm^2.

3.2. Equipment and Instrumentation

The major equipment and instrumentation used for testing the cube and beam specimens prepared for this study include: (i) Universal Testing Machine, (ii) Avongard standard tell-tale crack monitor, (iii) Linear Variable Displacement Transducer (LVDT) or dial gauges, and (iv) strain gauges. Other equipment used for material characterization include: (i) Genius IF for X-ray Fluorescence (XRF) analysis, (ii) TGA 4000 for Thermogravimetric Analysis (TGA), and (iii) Rigaku Miniflex 600 for X-ray Diffraction (XRD) analysis.

3.3. Tests and Characterization of Materials

Tests were conducted on three sand samples, granite, and cement to evaluate the compressive strength, durability, and compositional properties of resulting concrete cubes for structural suitability. The research assessed material quality to ensure compliance with reinforced concrete standards.

3.3.1. Tests on fine aggregates

Particle size distribution and determination of coefficient of curvature

Particle size distribution test was carried out according to the British Standard. The coefficient of curvature, shows the corresponding curve of particle size distribution for the aggregates used. These were calculated and categorized according to British Standard using Equations 1 and 2.

$$\text{Uniformity coefficient } C_u = \frac{D_{60}}{D_{10}} \tag{1}$$

$$\text{Coefficient of gradation } C_c = \frac{{D_{30}}^2}{D_{60} \times D_{10}} \tag{2}$$

Where:
D_{60} is the diameter of soil particles for which 60% are finer and 40% are coarser
D_{30} is the diameter of soil particles for which 30% are finer and 70% are coaser
D_{10} is the diameter of soil particles for which 10% are finer and 90% are coarser

The fineness modulus and silt content tests

These tests were carried out on fine aggregate according to British Standard procedures, which determines whether the aggregate is fine, and also ensure the aggregate cleanliness because excessive silt reduces bonding.

Moisture content determination

The moisture content of the aggregates used was determined in accordance with British standard. For the concrete grade, the test allowed adequate water-cement ratio for the concrete using Equation 3.

$$\text{Moisture content , MC } = \frac{W_{wet} - W_{dry}}{W_{dry}} \; x \; 100 \tag{3}$$

Slump test and compacting factor tests

The slump test, performed according to BS EN 12350-2:2009, measured the consistency of the fresh concrete. The results (50–90 mm) are adequate, fitting the 0.85–0.92 relative compaction range required for lightly reinforced sections without vibration or heavily reinforced sections with vibration, depending on the concrete's workability class. The compacting factor test is a measure of the workability of concrete. The compacting factor (CF) is defined as in Equation 4.

$$C\ F = \frac{Weight\ of\ partially\ compacted\ concrete\ (Wp)}{Weight\ of\ fully\ compacted\ concrete\ (Wf)} \tag{4}$$

Compressive strength test

The compressive strength test was carried out according to BS EN 12390-3:2019 on concrete cubes of size 150 mm × 150 mm × 150 mm. The cube samples were cured by immersion in water in a curing tank at temperature of 27℃ for curing period of 28 days. At 7th, 14th, 21st and 28th day. The cube was placed centrally on universal testing machine (UTM) platen by applying continuous load until the cube failure occurred, which determines their concrete compressive strength that determine samples load-bearing capacity, and it was calculated using Equation 5.

$$Compressive\ Strength = \frac{Failure\ Load\ (P)}{Cross - Sectional\ Area\ (A)} \tag{5}$$

The acceptance criteria for compressive strength test, is at 7-day strength, concrete strength should achieve 60-70% of its 28-day strength. While at 28-day, strength should match the design mix strength.

X-ray fluorescence (XRF) test

X-ray Fluorescence (XRF) test was used to determine the elemental composition of the fine aggregate sample, specifically for chemical analysis, and it was carried out according to BS EN 196-2:2013.

X-ray diffraction (XRD) test

X-ray Diffraction (XRD) test was used to determine the. structural information about crystal structure, lattice parameters, grain size, and other structural parameters, with XRD test carried out its analysis was to characterize the material which is in accordance with British standard.

Thermogravimetric analysis (TGA) of concrete

Thermogravimetric Analysis (TGA) was conducted on concrete made from three sand types. Moisture-free core samples were crushed to fine powder, organic matter removed, weighed, and analyzed using a calibrated TGA instrument with controlled heating rate and purge gas. Mass loss was recorded against temperature, and decomposition stages with corresponding percentage losses were identified. Results were interpreted based on concrete phases and compared with Differential Scanning Calorimetry (DSC) data. All tests complied with ASTM E1131:2014.

4. Results and Discussion

4.1. Mechanical Properties

4.1.1. Particle size distribution and determination of coefficient of curvature

Particle size distribution was conducted in accordance with BS EN 1097-5:2008. The sand sample was oven-dried, weighed, and sieved through standard sieve sizes using a mechanical shaker. The mass retained on each sieve was recorded, and corresponding percentages retained, cumulative retained, and percentage passing were calculated.

Table 1 Gradation Analysis of Sand Samples

SN	Diameter of Sand Particle (mm)	Sample A	Sample B	Sample C
1	D_{60}	0.400	1.100	0.400
2	D_{30}	0.190	0.500	0.350
3	D_{10}	0.000	0.250	0.000

The uniformity coefficient and coefficient of gradation can be calculated only for sand sample B as D_{10} for samples A and C results in zero value. The C_u for sample A is zero, sample B is 4.4, and sample C is zero. The sand sample B is a well graded sample, because when C_u is greater than 4, the sand sample is regarded as well graded sand and regarded as poorly graded or uniformly graded if sand is less than 4.

Based on the coefficient of gradation C_c, the sand is classified as well graded sand if, C_c in the range of 1 to 3. The coefficient of curvature C_c for sand sample B is 1.00, and that of sample A and C is zero. While the coefficient of uniformity Cu is for sample B is 4.40. These values indicate that the sand is well graded, since it is within the satisfactory range of 1 and 3 for coefficient of curvature, as specified by the British Standard BS812-1031:1989.

4.1.2. The fineness modulus and clay and silt content tests on fine aggregates

These tests were carried out on fine aggregate according to British Standard BS 812-103.1:1989. The fineness modulus of fine aggregates is calculated by summing the cumulative percentages of aggregate retained on the standard sieves sizes (5mm, 2.36mm, 1.18mm, 0.500mm, 0.212mm, and 0.150mm) and dividing the sum by 100, and percentage fine are as shown in Equations 6 and 7.

$$Fineness\ Modulus\ (FM) = \frac{\Sigma(Cumulative\ Percentage\ Weight\ Retained)}{100} = \quad (6)$$

$$Percentage\ Fines\ (Clay\ and\ Silt)\ (\%) = \frac{Weight\ in\ Pan}{Total\ weight} \quad = \qquad (7)$$

Table 2 Fineness Modulus for fine aggregates Physical properties of the sand samples.

Description	**Sample A**	**Sample B**	**Sample C**
Initial weight of sample (g)	200	200	200
Σ(Cumulative percentage weight retained) (g)	191.85	378.85	229.05
Fineness modulus (FM)	1.92	3.79	2.29
Clay and Silt Content (%)	17.50	4.95	11.90

The Sample B fine aggregate is well graded with a uniformity coefficient of 4.4 and coefficient of gradation of 1.0. The fineness modulus of 3.79 indicates a coarse sand, also the percentage fines which consists of both silt and clay content is 4.95% which is within the standard limit of 5 to 8%. The grading characteristics show that the sand is suitable for use in structural concrete production, particularly where high strength and reduced shrinkage are required.

4.1.3. Compressive strength test of Concrete Cubes

The compressive strength test was carried out according to BS EN 12390-3:2019 on concrete cubes of size 150mm × 150mm × 150mm. The compressive strength tests on different samples of concrete cubes, were taken at 7^{th} day, 14^{th} day, 21^{st} day and 28^{th} day respectively. The test is used to determine the quality of concrete whether it is in order with the proposed mix design carried out before the test. The equation for calculating the compressive strength of concrete is shown in Equation 5. The results of compressive strength carried out on sample A at 7^{th} day, 14^{th} day, 21^{st} day and 28^{th} day respectively are shown in Figures 2 to 5.

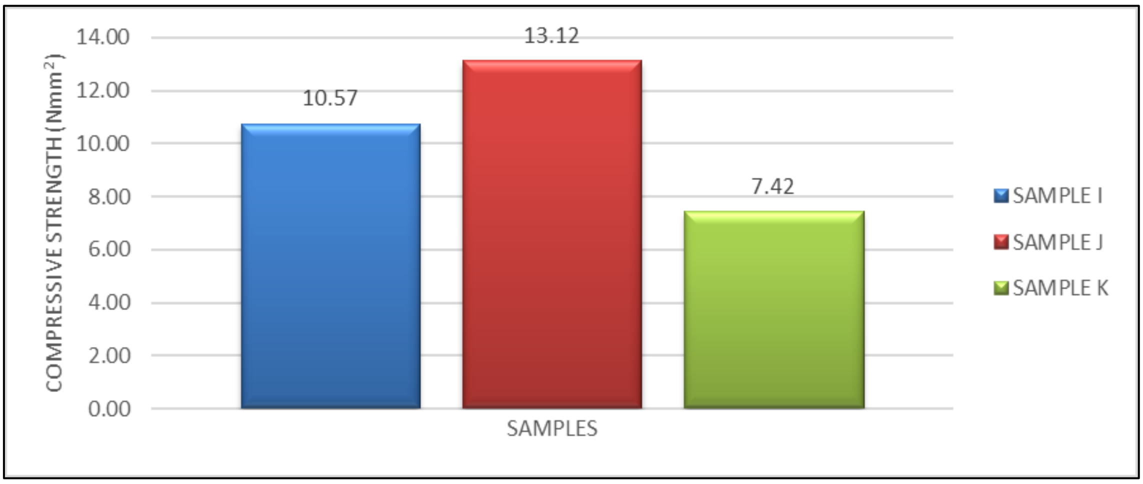

Figure 2 Bar Chart Showing Average Compressive Strength of Concrete Samples at 7 days

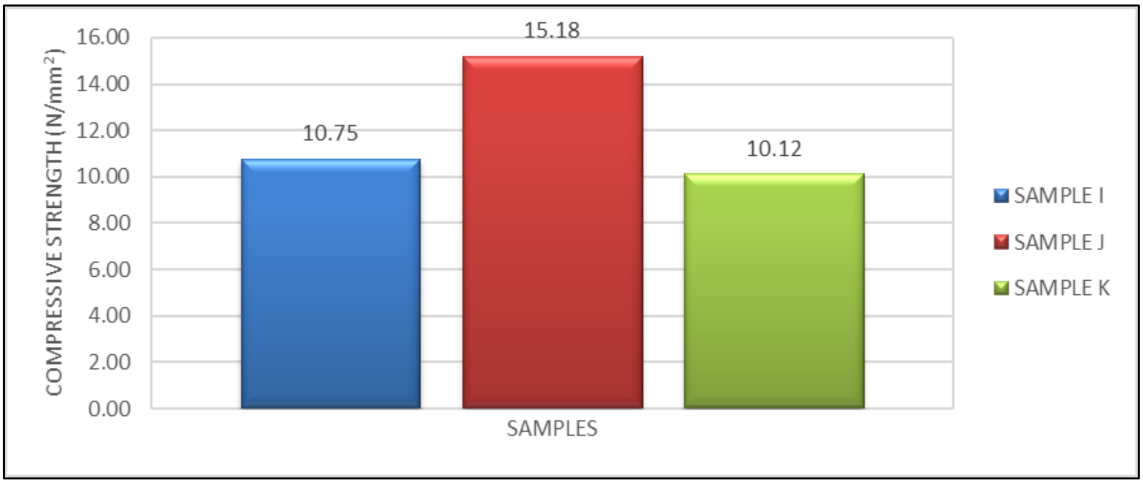

Figure 3 Bar Chart Showing Average Compressive Strength of Concrete Samples at 14 days

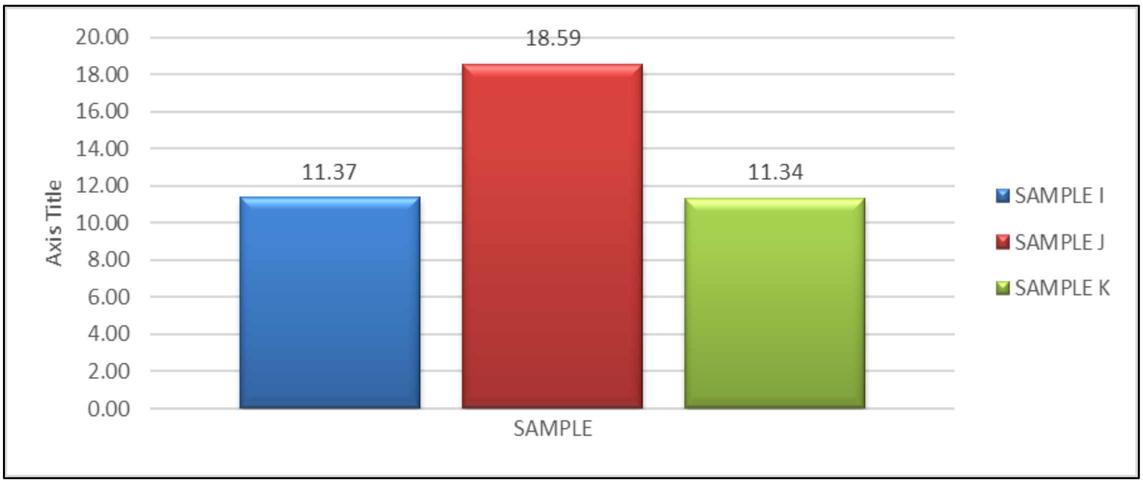

Figure 4 Bar Chart Showing Average Compressive Strength of Concrete Samples at 21 days

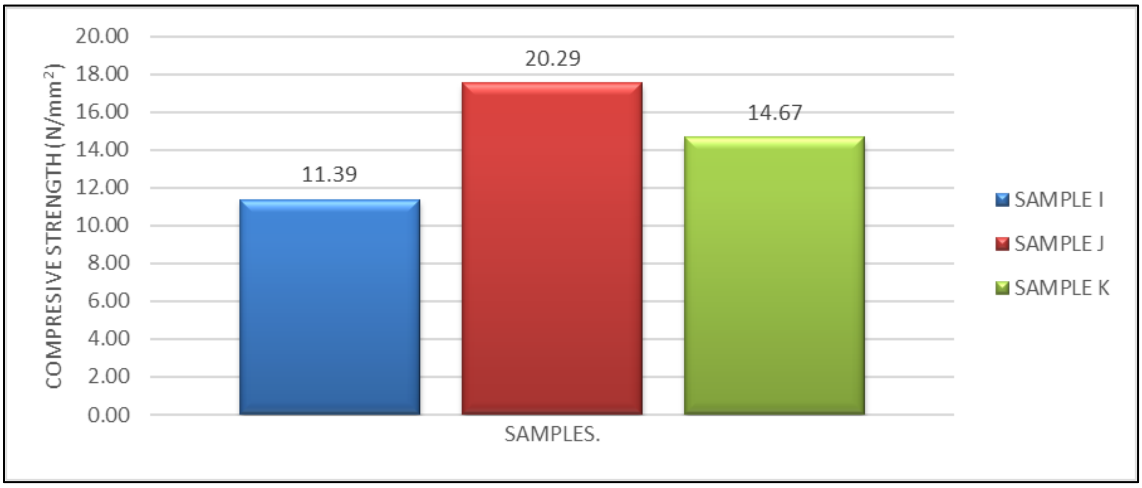

Figure 5 Bar Chart Showing Average Compressive Strength of Concrete Samples at 28 days

The compressive test results in Tables 4.45, 4.46, 4.47, and 4.48 indicate that concrete sample J from sand sample B is the strongest material with the lowest water absorption, while concrete sample I from sand sample A is the weakest with the highest water absorption for 7th day, 14th days, 21st day, and 28th day. Concrete sample J from sand sample B has the highest density (2504.15 kg/m^3) and lowest % water absorption (1.58%), followed by Sample K from sand sample C, then sample I from sand sample A (highest absorption: 2.92%; lowest density: 2387.26 kg/m^3) at 28th day. Compressive Strength Correlation shows there is a clear inverse relationship between water absorption and compressive strength. Concrete sample J exhibits the highest compressive strength (20.29 N/mm^2), corresponding to its minimal water absorption. Conversely, concrete sample I from sand sample A, with the highest water absorption, records the lowest strength (11.39 N/mm^2). This suggests that increased water content or absorption capacity compromises the material's structural integrity. The results highlight the critical role of material density and water sensitivity in determining mechanical performance. Materials with lower porosity or better packing (higher density) absorb less water and can withstand significantly higher loads. These findings suggest concrete sample J is the most suitable for applications requiring high structural integrity and water resistance, such as in concrete or stabilized earth construction, while Sample I may be less durable in moist environments. The test results identify concrete sample J from sand sample B has the highest performing concrete mix.

4.2. Characterization of Concrete Materials using Analytical Techniques

The concrete materials and concrete samples were characterized using analytical techniques such as, X-ray Fluorescence (XRF) test, X-Ray diffraction (XRD) test and Thermogravimetric Analysis (TGA) test to analyze the properties, composition, and structure of materials.

4.2.1. X-Ray fluorescence (XRF) tests

XRF is used for elemental composition analysis. It identifies compound oxides, elements present and quantifies the concentration in terms of weight percent (wt.%) and mole percent (mole %) of chemical elements present in a material by measuring the characteristic fluorescent X-rays that are emitted when a sample is excited by high-energy X-rays. The summary results of XRF test carried out on sand samples A, B, and C are presented in Table 3, which contains the output from the Genius IF machine used for the experiment and subsequent analysis

Table 3 X-Ray Fluorescence Test Raw data on Sand Samples A, B, and C

Layer	Component	Type	Concentration			Units
			Sample A	Sample B	Sample C	
Major Oxide						
1	SiO_2	Calc	66.837	73.551	73.709	wt.%
1	Fe_2O_3	Calc	4.485	2.404	3.282	wt.%
1	SO_3	Calc	3.420	5.762	1.726	wt.%
1	CaO	Calc	7.532	4.537	2.730	wt.%
1	MgO	Calc	0.000	0.000	1.229	wt.%
1	K_2O	Calc	1.861	4.066	3.579	wt.%
1	Al_2O_3	Calc	9.295	5.754	8.784	wt.%
1	TiO_2	Calc	3.391	1.570	1.681	wt.%
1	Cl	Calc	1.432	1.348	1.605	wt.%
Minor Oxides						
1	MnO	Calc	0.219	0.082	0.192	wt.%
1	CuO	Calc	0.131	0.085	0.127	wt.%
1	ZrO_2	Calc	0.767	0.404	0.420	wt.%
Trace Elements (Impurities)						
1	V_2O_5, Cr_2O_3	Calc	< 0.1	< 0.1	< 0.1	wt.%
	CoO, NiO, etc					

XRF analysis shows all samples are predominantly siliceous (SiO_2), making them generally suitable for concrete. Sample A has the highest Al_2O_3 (up to 9.30%) and CaO, potentially increasing water demand and alkali–aggregate reaction risk, though CaO can aid early strength. Samples B and C are cleaner with higher silica; however, Sample B's highest SO_3 and K_2O may reduce durability in sulfate environments. The role of the compound present in the sand sample B is as follows; the SiO_2 with weight % of 73.551% concentration, main component of siliceous quartz sand, which is a typical of good quality fine aggregate which, contributes to strength, durability and it is excellent for concrete. The Al_2O_3 with weight % of 5.754% concentration, enhances resistance to chemical attack, which affects setting time and common in clay minerals.

Table 4 X-Ray Fluorescence Test Raw data on Concrete Samples I, J, and K

Layer	Component	Type	Concentration			Units
			Sample A	Sample B	Sample C	
Major Oxide						
1	SiO_2	Calc	44.803	47.474	38.664	wt.%
1	Fe_2O_3	Calc	6.746	6.093	4.982	wt.%
1	SO_3	Calc	1.587	2.523	2.227	wt.%
1	CaO	Calc	26.522	27.207	40.201	wt.%
1	MgO	Calc	0.000	0.000	0.000	wt.%
1	K_2O	Calc	7.571	4.820	3.185	wt.%
1	Al_2O_3	Calc	9.532	8.861	7.538	wt.%
1	TiO_2	Calc	1.214	1.250	1.073	wt.%
1	Cl	Calc	0.532	0.552	0.665	wt.%
Minor Oxides						
1	MnO	Calc	0.138	0.086	0.090	wt.%
1	CuO	Calc	0.068	0.046	0.064	wt.%
1	ZrO_2	Calc	0.217	0.190	0.206	wt.%
Trace Elements (Impurities)						
1	V_2O_5, Cr_2O_3	Calc	< 0.1	< 0.1	< 0.1	wt.%
1	CoO,NiO, etc					

XRF analysis indicates that concrete Samples I, J, and K are dominated by SiO_2, CaO, and Al_2O_3 over 75% of the composition, making them suitable for structural use. Sample J has 47.47% SiO_2 suggests the best strength due to superior siliceous aggregates. Sample K (40.20% CaO) indicates the highest cement content but increased sulfate risk. Sample I exhibits the highest Fe_2O_3 and K_2O, suggesting darker color and greater ASR risk. SO_3 levels remain within acceptable limits for all samples. Overall, Sample J offers the most balanced composition for strength and durability. The samples are ranked as follows: Sample J next by Sample K and Sample I.

4.2.2. X-Ray diffraction (XRD) tests

XRD is used on material sample to determine its crystalline structure and phase composition by analyzing how X-rays are scattered by the material. It provides information on the arrangement of atoms and crystalline phases present in a sample. The XRD test carried out on sand and concrete samples present the list of mineral phase identified, qualitative analysis results are in Tables 5 and 6.

Table 5 X-Ray Diffraction (XRD) Qualitative Analysis and Phase Concentration Results of Sand Samples A, B, and C

No	Phase Name	Formula	Figure of merit			Dataset / Weight Fraction, wt.%		
			Sample A	Sample B	Sample C	Sample A	Sample B	Sample C
1	Orthoclase	$Al_2O_3K_2O6SiO_2$	3.168	3.265	1.969	16(3)	23(13)	16.9(19)
2	Albite	$NaAlSi_3O_8$	3.145	3.336	2.992	27(3)	3(5)	11.0(8)
3	Quartz, syn	SiO_2	1.752	1.521	1.643	48(3)	64(13)	70(3)
4	Goethite	FeO(OH)	3.274	3.182	2.093	8.2(12)	7(7)	1.1(2)
5	Muscovite	$H_2KAl_3(SiO_4)_3$	3.349	3.043	3.125	0.3(6)	3(4)	1.3(13)

Table 6 X-Ray Diffraction (XRD) Qualitative Analysis and Phase Concentration Results of Concrete Samples I, J, and K

No	Phase Name	Formula	Figure of merit			Dataset / Weight Fraction, wt.%		
			Sample I	Sample J	Sample K	Sample I	Sample J	Sample K
1	Orthoclase	$Al_2O_3K_2O6SiO_2$	3.226	2.850	3.145	14(10)	13.9(13)	43(18)
2	Albite	$NaAlSi_3O_8$	2.850	3.093	2.770	33(4)	8(6)	14(4)
3	Quartz, syn	SiO_2	1.121	0.963	1.276	39(5)	63(5)	42(14)
4	Calcite, syn	$CaCO_3$	2.750	2.750	3.449	4.2(5)	6.1(6)	1.1(19)
5	Muscovite	$H_2KAl_3(SiO_4)_3$	2.770	2.770	0.000	9.2(11)	8.4(8)	0.00

XRD analysis results in Table 5 reveals all sand samples are primarily Quartz (SiO_2), with Sample C with 70 wt.% exhibiting the highest purity and suitability for structural concrete, followed by Samples B (64 wt.%) and A (48 wt.%). Moderate Orthoclase and Albite contribute to durability, while trace Goethite and Muscovite are present. Table 6 indicates concrete samples I, J, and K contain Quartz, Feldspars, and low Calcite ranging from 1.1 to 6.1%, with Sample J being most siliceous and Sample K exhibiting high K-feldspar (43%). Figure of Merit values of 0.963 to 3.449 confirm high reliability for Quartz and moderate certainty for Calcite.

4.2.3. Thermogravimetric analysis (TGA) tests

Thermogravimetric analysis (TGA) is a thermal analysis technique used on a material sample to determine its mass change as a function of temperature and time in a controlled atmosphere. This provides key information about the material's properties and behavior under heat.

Thermogravimetric analysis (TGA) test on Sand Samples A, B, and C

The analysis of samples depends on two data; derivative thermogravimetric analysis (DTA) and thermogravimetric analysis (TGA). The DTA data is used to plot curve of derivative weight% (%/min) versus temperature (°C), where the rate of weight loss is tracked as temperature increases. and the TGA data is used to plot curve of weight% (%) versus temperature (°C), in order to analyze the changes in the sample due to heat.

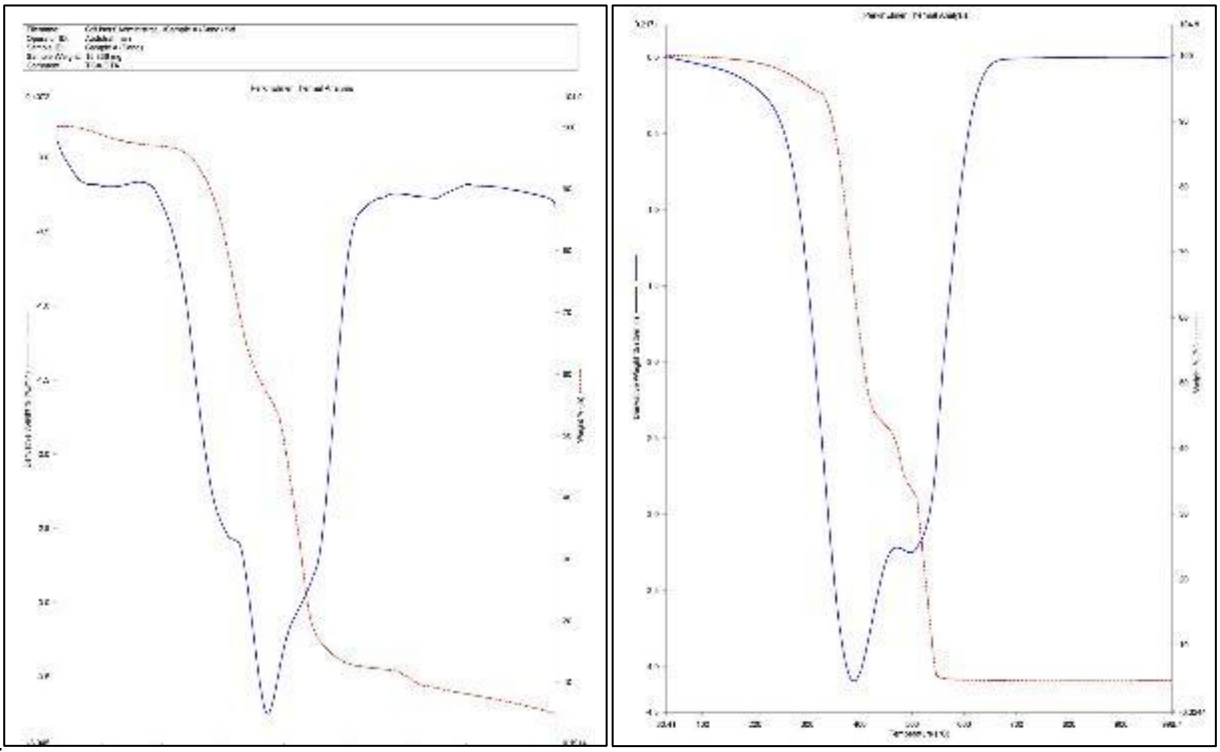

Figure 6 Overlay of TGA and DTA curves for Sand Samples A and B

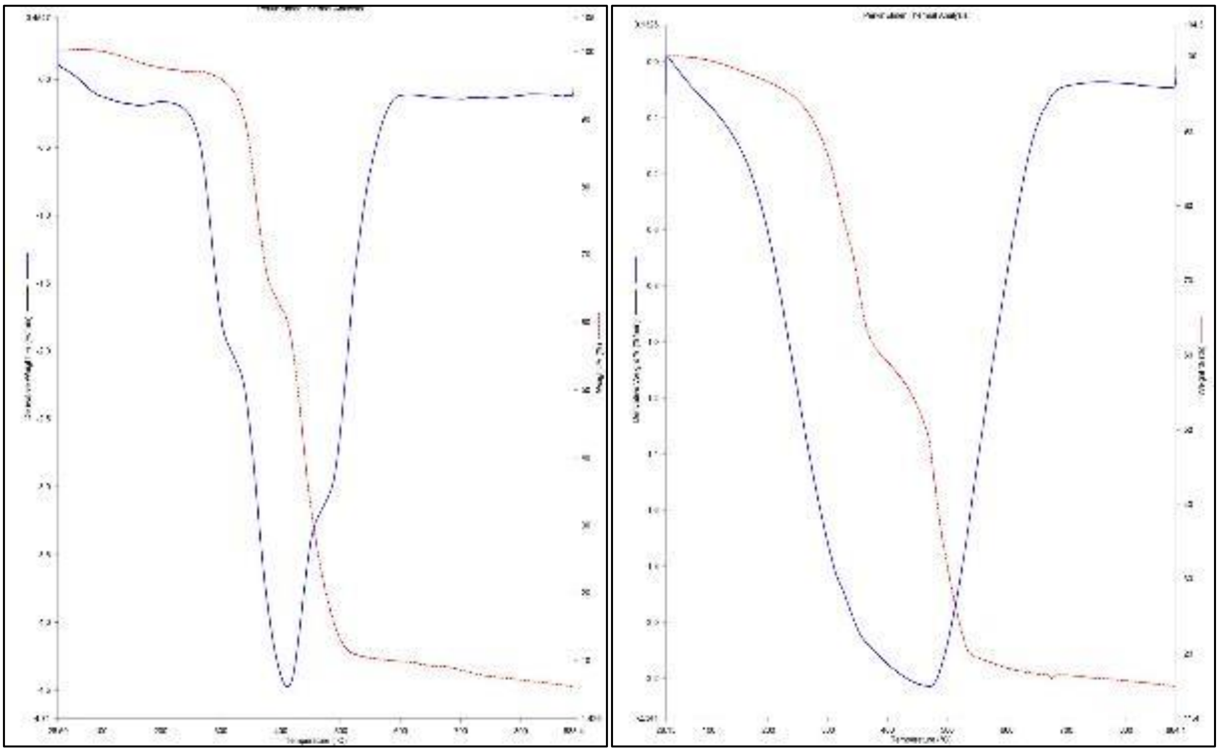

Figure 7 Overlay of TGA and DTA curves for Sand Sample C and Concrete Sample I

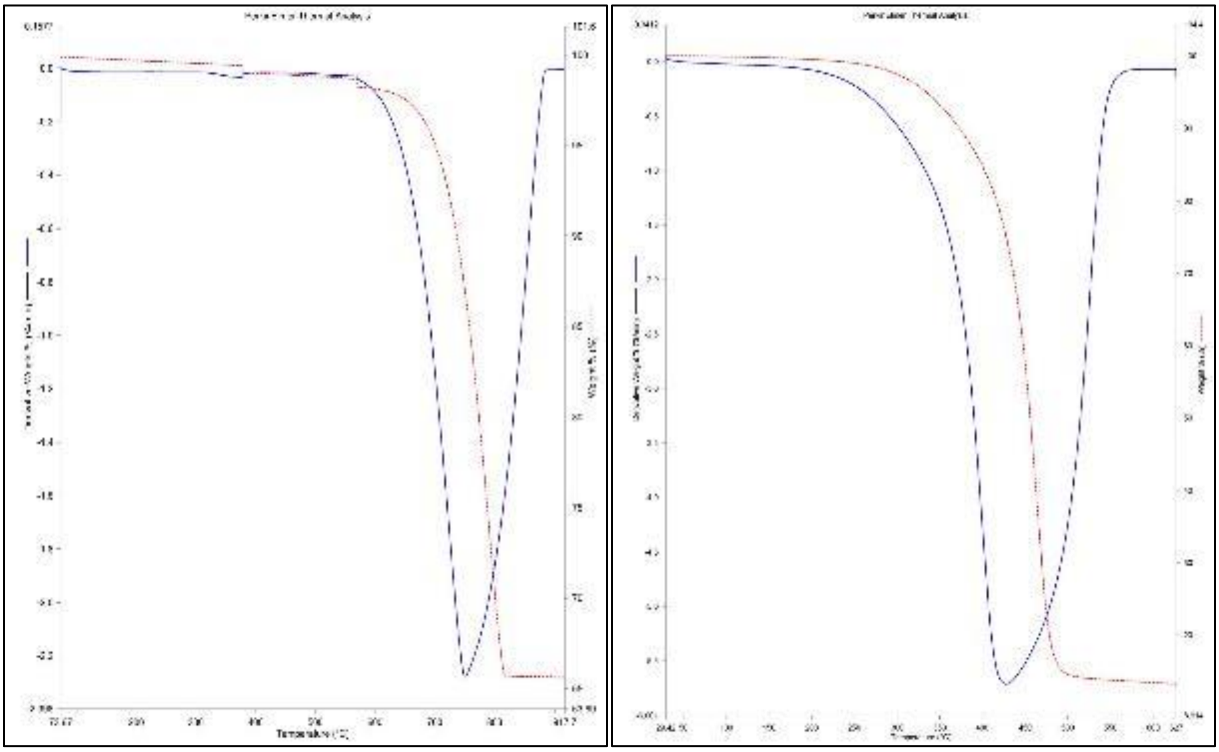

Figure 8 Overlay of TGA and DTA curves for Concrete Samples J and I

The overlay curves for samples are shown in Figures 6 and7 give clear insight into how to determine the total weight loss, residual mass, total mass loss in specific intervals, and estimate relative intensity of weight loss across temperature ranges from the overlay curve. The plot detail shows Temperature (°C) on the X-axis, on the left Y- axis DTG curve showing derivative weight % and on the right Y – axis TGA curve showing weight %. Overlay curves are plotted together to visualize decomposition phases and peak loss rates, while TGA curve is the red colour and DTG blue colour. The decomposition phases of the sample using derivative weight % to estimate relative intensity of weight loss across the temperature ranges. The change (Δ) derivative weight % value is calculated using Equation 8 and relative intensity estimate using Equation 9.

$$\Delta\ Derivative\ weight\ \% = Final - Initial \quad (8)$$

$$Relative\ Intensity\ Estimate = \frac{|\Delta\ derivative\ weight\ \%\ |}{Max\ (|\Delta deiivative\ weight\ \%|)} \quad (9)$$

The TGA curve data were used to quantify the mass loss at a specific interval for the decomposition phases of the sample for specific temperature intervals using weight % data. The mass loss was computed using Equation 10 the weight loss intensity, is calculated using Equation 11.

$$Total\ weight\ loss\ (\%) = Initial\ weight(\%) - Final\ weight(\%) \quad (10)$$

$$Weight\ loss\ intensity = \frac{Mass\ Loss\ (\%)}{Temperature\ Change\ (\Delta T)} \quad (11)$$

TGA analysis shows all three samples are mainly volatile or organic, with total mass loss ranging 93.87–95.51%. Sample B is the most decomposable (95.51% loss, 4.488% residual), while Sample C is the most thermally stable (93.87% loss, 6.134% residual). Peak weight loss rates occur at 373.96°C (Sample A, -3.746 %/°C), 389.79°C (Sample B, -4.094 %/°C), and 412.55°C (Sample C, -4.474 %/°C), confirming Sample C's superior thermal resistance. The residual mass reflects inorganic content, 4.5–6.0%. Overall, Sample C is best for durable concrete per BS standards, Sample B is suitable for general use, and Sample A is less favorable due to early thermal degradation.

Table 7 Comparative Results of TGA and DTG Analysis for Sample A, B, and C

SN	Description	Weight %		Total Mass Loss (%)	Final Residual Mass	Peak Loss Rate (%/?)	
		Initial	Final			Weight	Temperature
1	Sample A	100.000	4.952	95.05	4.952	-3.746	373.96
2	Sample B	100.000	4.488	95.51	4.488	-4.094	389.79
3	Sample C	100.000	6.134	93.87	6.134	-4.474	412.55

Thermogravimetric analysis (TGA) test on Concrete Samples I, J, and K (From Sand Sample A, B, and C)

The analysis of samples depends on two data; derivative thermogravimetric analysis (DTA) and thermogravimetric analysis (TGA). The DTA data is used to plot curve of derivative weight% (%/min) versus temperature (°C), where the rate of weight loss is tracked as temperature increases. and the TGA data is used to plot curve of weight% (%) versus temperature (°C), in order to analyze the changes in the sample due to heat. The overlay curves for concrete samples I, J, and K are shown in Figures 7 and 8.

Table 8 Comparative Results of TGA and DTG Analysis for Concrete Sample I, J, and K (From Sand Samples A, B, and C)

SN	Description	Weight %		Total Mass Loss (%)	Final Residual Mass	Peak Loss Rate (%/?)	
		Initial	Final			Weight	Temperature
1	Sample I	100.000	15.621	84.38	15.621	-2.227	473.33
2	Sample J	100.000	65.603	34.40	65.603	-2.081	743.32
3	Sample K	100.000	13.252	86.75	13.252	-5.712	428.64

TGA analysis of concrete samples I, J, and K (from sand samples A, B, and C) shows they are largely volatile or organic. Sample K (sand C) is the most decomposable with 86.75% mass loss and 13.25% residual, while Sample J (sand B) is most thermally stable, losing only 34.40% and retaining 65.60%. Peak weight loss rates occur at 473.33 °C (-2.227 %/°C, Sample I), 743.32 °C (-2.081 %/°C, Sample J), and 428.64 °C (-5.712 %/°C, Sample K), confirming Sample J's superior thermal resistance. Residual mass reflects inorganic content (13–65%). Engineering implications indicate Sample J offers the highest durability and fire resistance, Sample I moderate, and Sample K the lowest, making Sample J most suitable for structural and fire-resistant concrete.

5. Conclusion

The study confirms that the mechanical and thermal performance of deep beams is strongly influenced by the properties of constituent materials, particularly fine aggregates. Sand Sample B, with a percentage clay and silt content value of 4.95% with fineness modulus of 3.79 shows that the relationship between the two are inversely proportional, and good gradation characteristics, produced Concrete Sample J, which exhibited the highest 28-day compressive strength (20.29 N/mm^2) and superior characteristic strength. XRF results showed high SiO_2 content (66–74%) in the sands and dominant CaO (75%) in cement, indicating proper chemical composition for strength development. XRD analysis revealed high quartz and orthoclase content in Sand B, contributing to improved mechanical performance. TGA/DTA results further demonstrated that Sample J possessed better thermal stability and resistance to high-temperature degradation. Therefore, material characterization significantly affects the load-bearing and strength behavior of reinforced concrete deep beams at limit state.

Recommendations

- Sand with good gradation and high quartz content (similar to Sample B) should be preferred for deep beam construction.
- Comprehensive material characterization (XRF, XRD, TGA) should be conducted before structural application.

- Concrete produced from well-graded coarse fine aggregates should be used for structural and fire-resistant deep beam applications.
- Further research should evaluate different loading configurations (point, distributed, dynamic loads) to enhance deep beam design optimization.

Compliance with ethical standards

Acknowledgments

We acknowledge The Federal University of Technology Akure Nigeria for granting us access to the Civil and Environmental Engineering Department Laboratory**.** Also to the Centre for Energy Research and Training, ABU Zaria where characterization of materials was carried out.

Disclosure of conflict of interest

No conflict of interest to be disclosed.

Statement of informed consent

Informed consent was obtained from all individual participants included in the study.

References

[1] Seena, P. and Chandran, A. (2021). Shear Strength of Reinforced Concrete Deep Beam. *Innovations in Civil Engineering, Conference paper Marian Engineering College.*

[2] Harsha, G. S. and Raju, P. P. (2019). Shear Strength of Deep Beams: A State of Art*. International Journal of Recent Technology and Engineering (IJRTE)*, *7(6C2); 2277-3878.*

[3] Engelsmann, S., Peters, S., Spalding, V. and Forstlechner, F. (2014). Designing structures with structural concrete. *Modern Concrete Construction Manual, 70-105.*

[4] Blikharskyy, Y., Selejdak, J., Vashkevych, R., Kopiika, N., and Blikharskyy, Y. (2023) Strengthening Reinforced Concrete eccentrically loaded columns by Concrete Fibre Reinforced Polymer at different levels of initial load. *Engineering Structures 280(5):115694.*

[5] Jian, C., Hang, H., and Yanchao, S. (2017). Discussion on the suitability of concrete constitutive models for high-rate response predictions of RC structures*. International Journal of Impact Engineering, 106: 202 – 216.*

[6] Guo, Y. (2021). Analysis on Concrete Construction Technology in Civil Engineering Construction. *Journal of Physics, doi:10.1088/1742-6596/2011/1/012023.*

[7] Guo, Z. (2014). Basic Mechanical Behavior. *Principle of Reinforced Concrete. 9-52. DOI:10.1016/B978-0-12-800859-1.00002-5.*

[8] Abtan, Y. and Hassan, F. (2020). A review of behavior of reinforced concrete deep beams. Journal of Engineering and Sustainable Development, 24(05).

[9] Fan, S., Zhang, Y. Ma, Y. X. and Tan, K. H. (2022). Strut-and-tie and finite element modelling of unsymmetrically-loaded deep beams. *Structures 36: 805–821.*

[10] Tan, K. H. Tang, C. Y. and Tong, K. (2003). A direct method for deep beams with web reinforcement. *Magazine of Concrete Research. 55 (1): 53–63.*

[11] Kadhim, H. K., and Abdullah, M. D. (2022). Effect of loading type in concrete deep beam with strut reinforcement. *Open Engineering, 14: 20220488*(2024).

[12] Neville, A. M. (2011). Properties of concrete 5th Edition. *Pearson Education Limited. ISBN 978.0-273-75356-6.*